

# InP-Based All-Epitaxial 1.3- $\mu\text{m}$ VCSELs With Selectively Etched AlInAs Apertures and Sb-Based DBRs

T. Asano, D. Feezell, R. Koda, M. H. M. Reddy, D. A. Buell, A. S. Huntington, E. Hall, S. Nakagawa, and L. A. Coldren, *Fellow, IEEE*

**Abstract**—We report, for the first time, InP-based all-epitaxially grown 1.3- $\mu\text{m}$  vertical-cavity surface-emitting lasers with lattice-matched Sb-based distributed Bragg reflectors and AlInAs etched apertures. The minimum threshold current and voltage under pulsed operation were 3 mA and 2.0 V, respectively. The thermal impedance was as low as 1.2 K/mW without heat sinking. Implementation of the AlInAs etched aperture was quite effective in improving the injection efficiency and reducing the internal loss, resulting in improved differential efficiency.

**Index Terms**—Optical fiber communication, quantum well lasers, semiconductor device fabrication, semiconductor lasers, surface-emitting lasers.

## I. INTRODUCTION

LONG-WAVELENGTH vertical-cavity surface-emitting lasers (VCSELs) emitting at 1.3  $\mu\text{m}$  are expected to provide economic benefits for optical communication systems because of their inherent advantages over edge emitters such as on-wafer testing, ease of coupling to a fiber, and the feasibility of two-dimensional arrays.

In this wavelength region, much attention has been paid to VCSELs with GaAs-based distributed Bragg reflector (DBR) mirrors which demonstrate high reflectivity and low thermal impedance. The best results in terms of maximum temperature for electrically pumped continuous-wave (CW) operation and reliability have been so far attained with GaAs-based VCSELs with GaInNAs active regions [1]–[6]. However, since the material quality and the lasing wavelength are very sensitive to nitrogen content, many of the good laser characteristics have been reported at wavelengths below 1.3  $\mu\text{m}$ . In addition, the uniformity of the lasing wavelength over the wafer and the run-to-run reproducibility are of some concern.

The other approach to realize 1.3- $\mu\text{m}$  VCSELs is to use InP-based technology. In this case, the lack of a suitable material combination to obtain high reflectivity DBRs and the lack of a reproducible aperturing technique such as oxidation of AlGaAs in GaAs-based VCSELs were major issues. However, we have previously demonstrated CW operation up to 88 °C for 1.55- $\mu\text{m}$  VCSELs, where newly developed Sb-based DBRs were used to provide high reflectivity and the active regions were selectively etched to form the current and optical apertures [7], [8]. Apart

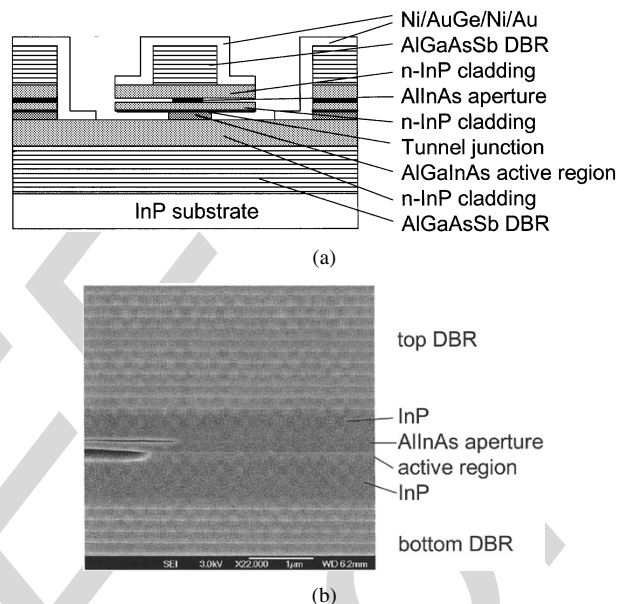


Fig. 1. (a) Schematic of VCSEL structure with undercut active region and thin etched AlInAs aperture. (b) Cross-sectional SEM of etched VCSEL structure.

from that, an InP double-intracavity contacted structure was also implemented to circumvent the poor electrical and thermal conductivity of the Sb-based DBRs [9].

One of the problems for further improvement of this intracavity contacted VCSELs is that the current tends to crowd around the edge of the active regions. This results in a weak overlap of the current and the optical mode, leading to the relatively low differential efficiency. The other problem is the scattering loss caused by  $1/2\lambda$ -thick undercut active regions [10]. In order to overcome these problems, a thin AlInAs etched aperture embedded in the InP cavity was introduced. Similar etched aperture structures for low loss have been reported in GaAs [11], [12]. In this letter, we report the fabrication and characterization of InP-based 1.3- $\mu\text{m}$  VCSELs with Sb-based DBRs and newly developed apertures. A comparison between the laser characteristics of the conventional structure and the new structure is also reported.

## II. EXPERIMENTAL

Fig. 1(a) shows a schematic of the 1.3- $\mu\text{m}$  VCSEL structure. This structure is based on the same design concept as our earlier reported 1.55- $\mu\text{m}$  VCSEL, except for the thin AlInAs etched

Manuscript received September 13, 2002; revised May 28, 2003.

The authors are with the Department of Electrical and Computer Engineering and Materials, University of California, Santa Barbara, CA 93106 USA.

Digital Object Identifier 10.1109/LPT.2003.817987

aperture enclosed in the InP cavity. One major advantage of this structure is that, by a slight adjustment of the layer thickness and Al content, both 1.3- and 1.55- $\mu\text{m}$  VCSELs can be realized using the same design and technology. The VCSELs were grown on undoped InP substrates using molecular beam epitaxy whose growth procedures were reported elsewhere [13]. The bottom and top DBRs, both lattice-matched to InP, consist of 24.5 and 35.5 pairs of undoped  $\text{Al}_{0.3}\text{Ga}_{0.7}\text{AsSb}$  and  $\text{Al}_{0.95}\text{Ga}_{0.05}\text{AsSb}$ , providing a reflectivity of 98.7% and 99.9%, respectively. A  $1/2\text{-}\lambda$ -thick active region, consisting of five compressively strained  $\text{AlGaInAs}$  quantum wells each 7 nm thick and 6 tensile-strained  $\text{AlGaInAs}$  barriers each 5 nm thick, is sandwiched by InP layers. The total cavity has an optical thickness of  $7/2\lambda$ . A tunnel junction consisting of highly p-doped  $\text{AlInAs}$  and highly n-doped InP was inserted between the active region and upper InP so as to eliminate absorption loss due to p-doped regions. The InP layers function as both current and heat spreading layers. A 30-nm-thick layer of  $\text{AlInAs}$  for the etched aperture was embedded in the upper InP layer. Ni–AuGe–Ni–Au was evaporated on both InP layers to form the top and bottom contacts.

The top DBR and InP were etched down to the  $\text{AlInAs}$  aperture layer by reactive ion etching (RIE) with  $\text{Cl}_2$  and  $\text{CH}_4\text{-H}_2\text{-Ar}$ , respectively. Subsequently, a selective lateral wet etching of the  $\text{AlInAs}$  aperture was carried out. Then, the remaining InP was etched using RIE, followed by a wet etching of the active region to expose the InP layer. Selective wet etching of both the thin  $\text{AlInAs}$  layer and the active region was performed to form the apertures using a mixture of citric acid and hydrogen peroxide [14].

In order to improve the overlap of the current and the optical mode, and to reduce the scattering loss by the undercut active regions, the diameter of the  $\text{AlInAs}$  aperture should be smaller than that of the active region. As can be seen from a cross-sectional scanning electron microscope (SEM) picture of a test VCSEL structure in Fig. 1(b), this condition is attained by our fabrication procedure. A careful inspection of the SEM picture also reveals that the top DBR has a wavy cross section due to a slight lattice mismatch, which is generally not present. Since this wavy interface might result in an increase in internal loss, further adjustment of the growth is required.

### III. RESULTS AND DISCUSSION

Fig. 2 shows the reflectivity spectrum of an as-grown VCSEL structure. As can be seen from the figure, the cavity mode is centered at 1.294  $\mu\text{m}$ . The large stop band of over 90 nm results from the large index contrast of Sb-based DBRs. Photoluminescence (PL), measured after removing the top DBR, showed the peak at 1.312  $\mu\text{m}$ . Unfortunately, the PL (gain) peak is at a longer wavelength than the cavity mode, which is the opposite of the desired gain-mode offset.

Fig. 3 shows the light output versus current and voltage versus current ( $L\text{-}I\text{-}V$ ) characteristics of a VCSEL with an 8- $\mu\text{m}$  diameter  $\text{AlInAs}$  aperture and a 9- $\mu\text{m}$  diameter active region under pulsed operation. The threshold current and the voltage at threshold were 3 mA and 2.0 V, respectively. The inset of Fig. 2 shows the emission spectrum and the lasing

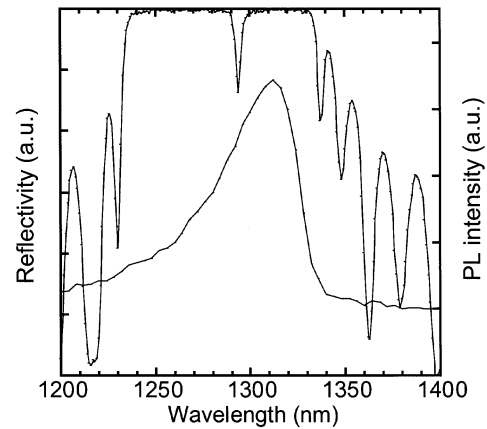


Fig. 2. PL and reflectivity spectra of VCSEL with Sb-based DBRs. PL was measured after removing the top DBR.

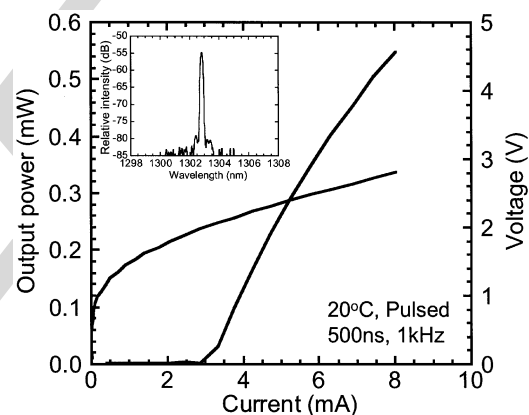


Fig. 3. Characteristics of a VCSEL with an 8- $\mu\text{m}$  undercut  $\text{AlInAs}$  aperture and a 9- $\mu\text{m}$  undercut active region under pulsed operation.  $L\text{-}I\text{-}V$  data was under-sampled yielding curve segmentation and giving apparent soft turn-on of  $L\text{-}I$  curve. Inset shows lasing spectrum.

wavelength was 1.303  $\mu\text{m}$ . CW operation at 5  $^\circ\text{C}$  was observed in spite of the misalignment between the cavity mode and gain peak and the wavy interface of the top DBR.

The thermal impedance was estimated from the temperature dependence of the lasing wavelength under pulsed operation and the cavity mode shift with the dissipated power. The result was as low as 1.2 K/mW without heat sinking. This value is comparable with that of GaAs-based VCSELs [3].

In order to confirm the effectiveness of the thin  $\text{AlInAs}$  aperture, we compared the laser characteristics of devices with and without the  $\text{AlInAs}$  aperture. Both VCSELs were fabricated from the same wafer, and both contained the undercut active regions. The aperture diameter of the VCSELs with the  $\text{AlInAs}$  aperture was adjusted to be 3  $\mu\text{m}$  smaller than the diameter of the undercut active regions. Fig. 4 shows the variation of the differential efficiency with the aperture diameter. In this figure, the effective aperture diameter refers to the diameter of the  $\text{AlInAs}$  aperture for the VCSELs with the  $\text{AlInAs}$  aperture, and to the active regions for the VCSELs without the  $\text{AlInAs}$  aperture. Maximum differential efficiency is obtained at an effective aperture diameter of 8  $\mu\text{m}$  for both VCSELs with and without  $\text{AlInAs}$  aperture. The VCSELs with  $\text{AlInAs}$  apertures show higher differential efficiency than those without  $\text{AlInAs}$

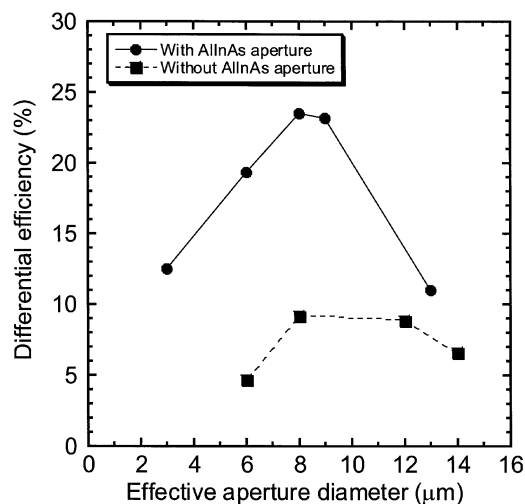


Fig. 4. Differential efficiency as a function of effective aperture diameter. Effective aperture diameter indicates the diameter of the AlInAs apertures for the VCSELS with AlInAs apertures and of the active regions for those without AlInAs apertures.

apertures at all aperture diameters. The maximum value was 23%. Therefore, the AlInAs aperture is quite effective in improving the differential efficiency.

The injection efficiency and internal loss of the apertured and unapertured VCSELS were calculated to more clearly understand the effects of the AlInAs aperture. These parameters were determined from the  $L$ - $I$  characteristics (i.e., differential efficiency and threshold current) of the devices. In this calculation, threshold gain was extracted by using the injection efficiency and gain curve of in-plane lasers with the same active region as that of the VCSELS [15]. As a result, an injection efficiency of 71% was obtained for the VCSEL with the AlInAs aperture. In contrast, the VCSEL without the AlInAs aperture had an injection efficiency of 51%. Both VCSELS had an effective aperture diameter of 8  $\mu\text{m}$ . This result indicates that the AlInAs aperture prevents the current from crowding around the edge of the active regions, leading to an improved current and optical mode overlap. Moreover, the internal loss for the VCSEL with the AlInAs aperture was found to be  $50 \text{ cm}^{-1}$  smaller compared with the one without the AlInAs aperture. We speculate that this is attributed to the reduced scattering loss from the thin AlInAs aperture. However, both numbers were higher than desired, probably because of the nonplanar DBR growth as mentioned above.

#### IV. CONCLUSION

1.3- $\mu\text{m}$  VCSELS with lattice-matched Sb-based DBRs and AlInAs etched apertures were epitaxially grown on InP and successfully fabricated. A minimum threshold current of 3 mA was obtained in spite of the misalignment of the gain and cavity

mode, and interfacial roughness of the top DBR. Measured thermal impedance was as low as 1.2 K/mW. Implementation of the thin AlInAs etched aperture improved the current and optical mode overlap, and reduced the scattering loss, leading to higher differential efficiency. These results indicate that this design and technology are very attractive for VCSELS within the 1.3–1.55- $\mu\text{m}$  range.

#### REFERENCES

- [1] K. D. Choquette, J. F. Klem, A. J. Fischer, O. Blum, A. A. Allerman, I. J. Fritz, S. R. Kurtz, W. G. Breiland, R. Sieg, K. M. Geib, J. W. Scott, and R. L. Naone, "Room temperature continuous wave InGaAsN quantum well vertical-cavity lasers emitting at 1.3  $\mu\text{m}$ ," *Electron. Lett.*, vol. 36, pp. 1388–1390, 2000.
- [2] S. Sato, N. Nishiyama, T. Miyamoto, T. Takahashi, M. Jikutani, M. Arai, A. Matsutani, F. Koyama, and K. Iga, "Continuous wave operation of 1.26  $\mu\text{m}$  GaInNAs/GaAs vertical-cavity surface-emitting lasers grown by metalorganic chemical vapor deposition," *Electron. Lett.*, vol. 36, pp. 2018–2019, 2000.
- [3] M. C. Larson, C. W. Coldren, S. G. Spruytte, H. E. Petersen, and J. S. Harris, "Low-threshold oxide-confined GaInNAs long wavelength vertical cavity lasers," *IEEE Photon. Technol. Lett.*, vol. 12, pp. 1598–1600, Dec. 2000.
- [4] L. R. Thompson, L. M. F. Chirovsky, A. W. Jackson, R. L. Naone, D. Galt, S. R. Prakash, S. A. Feld, M. V. Crom, J. G. Wasserbauer, M. D. Lange, B. Mayer, and D. W. Kisker, "Performance of monolithic 1.3  $\mu\text{m}$  VCSELS in telecom applications," *Proc. SPIE*, vol. <AUTHOR: PLEASE PROVIDE VOLUME>, pp. 25–30, 2002.
- [5] C. S. Murray, F. D. Newman, S. Sun, J. B. Clevenger, D. J. Bossert, C. X. Wang, H. Q. Hou, and R. Stall, "Development of 1.3 micron oxide-confined VCSELS grown by MOCVD," *Proc. SPIE*, vol. <AUTHOR: PLEASE PROVIDE VOLUME>, pp. 30–38, 2002.
- [6] A. Ramakrishnan, G. Steinle, D. Supper, C. Degen, and G. Ebbinghaus, "Electrically pumped 10 Gbit/s MOVPE-grown monolithic 1.3  $\mu\text{m}$  VCSEL with GaInNAs active region," *Electron. Lett.*, vol. 38, pp. 322–324, 2002.
- [7] E. Hall, S. Nakagawa, G. Almuneau, J. K. Kim, and L. A. Coldren, "Room-temperature, CW operation of lattice-matched long-wavelength VCSELS," *Electron. Lett.*, vol. 36, pp. 1465–1467, 2000.
- [8] S. Nakagawa, E. Hall, G. Almuneau, J. K. Kim, D. A. Buell, H. Kroemer, and L. A. Coldren, "88  $^{\circ}\text{C}$ , continuous-wave operation of apertured, intracavity contacted, 1.55  $\mu\text{m}$  vertical-cavity surface-emitting lasers," *Appl. Phys. Lett.*, vol. 78, pp. 1337–1339, 2001.
- [9] —, "1.55- $\mu\text{m}$  InP-lattice-matched VCSELS with AlGaAsSb-AlAsSb DBRs," *IEEE Select. Topics Quantum Electron.*, vol. 7, pp. 224–230, Mar./Apr. 2001.
- [10] E. R. Hegblom, D. I. Babic, B. J. Thibeault, and L. A. Coldren, "Estimation of scattering losses in dielectrically apertured vertical cavity lasers," *Appl. Phys. Lett.*, vol. 68, pp. 1757–1759, 1996.
- [11] J. W. Scott, B. J. Thibeault, D. B. Young, L. A. Coldren, and F. H. Peters, "High efficiency submilliamp vertical cavity lasers with intracavity contacts," *IEEE Photon. Technol. Lett.*, vol. 6, pp. 678–680, June 1994.
- [12] G. S. Li, S. F. Lim, W. Yuen, and C. J. Chang-Hasnain, "Polarization and modal behavior of low threshold oxide and airgap confined vertical cavity lasers," *Electron. Lett.*, vol. 31, pp. 2014–2015, 1995.
- [13] G. Almuneau, E. Hall, S. Nakagawa, J. K. Kim, D. Lofgreen, O. Sjolund, C. Luo, D. R. Clarke, J. H. English, and L. A. Coldren, "Molecular beam epitaxial growth of monolithic 1.55  $\mu\text{m}$  vertical cavity surface emitting lasers with AlGaAsSb/AlAsSb Bragg mirrors," *J. Vac. Sci. Technol. B.*, vol. 18, pp. 1601–1604, 2000.
- [14] E. Hall, S. Nakagawa, G. Almuneau, J. K. Kim, and L. A. Coldren, "Selectively etched undercut apertures in AlAsSb-based VCSELS," *IEEE Photon. Technol. Lett.*, vol. 13, pp. 97–99, Feb. 2001.
- [15] L. A. Coldren and S. W. Corzine, *Diode Lasers and Photonic Integrated Circuits*. New York: Wiley, 1995, ch. 2.